PAQR3 controls autophagy by integrating AMPK signaling to enhance ATG14L-associated PI3K activity

Da-Qian Xu, Zheng Wang, Chen-Yao Wang, De-Yi Zhang, Hui-Da Wan, Zi-Long Zhao, Jin Gu,Yong-Xian Zhang, Zhi-Gang Li, Kai-Yang Man, Yi Pan, Zhi-Fei Wang, Zun-Ji Ke, Zhi-Xue Liu, Lu-Jian Liao, and Yan Chen

Appendix

Table of contents

Appendix Materials and Methods

Plasmids and short hairpin RNA (shRNA)

Full-length human VPS15, Beclin1 (untagged), Flag-tagged VPS34, Flag-tagged UVRAG, GFP-fused ATG14L, GFP-fused DFCP1 were purchased from Addgene (Cambridge, MA, USA). Among these plasmids, VPS15, ATG14L and Beclin1 were sub-cloned into p3Xflag-CMV-10 vector (Sigma-Aldrich, St. Louis, MO, USA). Beclin1 was also inserted into pRK-5 mammalian expression vector (BD biosciences) with a GST tag added to the N-terminus by a PCR-based method. Plasmids of the Flag-tagged AMPKα1 as well as its dominant negative (DN) and constitutive active (CA) forms were provided by Dr. Yu Li (Institute for Nutritional Sciences, SIBS, CAS, China). For mapping their interaction domains with PAQR3, diverse truncations of ATG14L and Beclin1 were inserted into EGFP-C1 vector. Myc-tagged PAQR3, and PAQR3-shRNA have been described as previously reported (Feng et al, 2007; Jiang et al, 2010; Zhang et al, 2010). Multiple PAQR3 deletions were sub-cloned into PCMV-tag3 vector by overlap extension PCR. For prokaryotic expression and purification, the NH_2-terminal 71 amino acids of PAQR3 (or multiple mutations) were inserted into the bacterial expression construct (PET28+). Point mutations of PAQR3 were performed by a PCR-based site-directed mutagenesis method using Pfu polymerase (Stratagene).

The lentivirus-based vectors pLVX-Puro and pHAGE-fullEF1a-MCS-IZsGreen were used for stable expression of GFP-DFCP1 and PAQR3 in HeLa cells respectively. The ATG5, ATG7 and ATG14L short hairpin RNA (shRNA) was constructed by a lentiviral system as previously reported (Qin et al, 2003). The sequences for constructing two independent shRNAs against human ATG14L were 5'-GGCAAATCTTCGACGATCCCATATA-3' and 5’-GATCACAACGGAGACACCAGCATTA-3’ respectively. The shRNA-resistant expression plasmid of ATG14L, PAQR3 and NRBF2 were constructed by same-sense mutations at the targeting sequence of their cDNA. Human ATG5 and ATG7 shRNA sequence were 5'-GGTTTGGACGAATTCCAACTTGTTT-3' and 5'-GCCGTCATTGCTGCAAGCAAGAGAA -3' respectively. The target sequences of

human PAQR3- and NRBF2-shRNAs were both reported previously (Zhang et al, 2010; Zhong et al, 2014). The expression plasmids used in the study were generated according to standard molecular biology techniques. All the plasmids were subjected to sequencing verification.

Cell culture, transfection, cell treatment, and viral Infection

HEK293T and HeLa cell lines were purchased form Cell Bank (Shanghai Institutes for Biological Sciences, CAS, China). HEK 293T, MEF and HeLa cell lines were maintained in normal medium (NM) containing high glucose (25 mM) DMEM (Invitrogen, #11965) medium containing 10% fetal bovine serum (FBS; Invitrogen) and 50 mg/ml penicillin/streptomycin. The method of MEF isolation from wild type and PAQR3-deleted mouse embryos was described previously (Feng et al, 2007). We generated PAQR3-deficient HeLa cells using a CRISPR/Cas9 system as previously reported (Cong et al, 2013; Mali et al, 2013). The sequences of two PAQR3-targetting guide RNAs were 5'-GAGCGCGCATTACATCGAGC-3' and 5'-CGTACATCACCGACGCTCTAC -3' respectively.

For glucose starvation (GS), the cells were cultured in the same medium as mentioned above except using the no-glucose DMEM (Invitrogen, #11966). Amino acid-free medium was prepared according to Gibco standard recipe by removing all amino acids and in dialysed FBS (Invitrogen). Transient transfection was performed using Polyjet (Signagen), lipofectamine 2000 (Invitrogen) or polyethylenime (Sigma-Aldrich) transfection reagents according to the manufacturer's instructions. AMPKα1/2 double knockout MEFs were kindly provided by Dr. Sheng-Cai Lin from Xiamen University, China. To establish the stably transfected cell lines, different lentivirus-based vectors were co-transfected with viral packaging plasmids (psPAX2 and pMD2.G) into HEK293T cells. Thirty hours after the transfection, the medium was collected and added to the target cells and the pools with stable expression of a gene of interest were obtained in the presence of 5 mg/ml puromycin (Sigma-Aldrich), followed by flow cytometry selection.

Antibodies and reagents

Antibodies used in the immunoblotting were as follows: LC3 (#2775), SQSTM1/p62 (#5114), phospho-4E-BP1 S65 (#9451), 4E-BP1 (#9452), VPS34 (#4263), Beclin1 (#3738), phospho-ACC S79 (#3661), ACC (#3662), phospho-AMPKα T172 (#2531), AMPKα (#2532), NRBF2 (#8633) and phospho-Beclin1 S93 (#14717) from Cell Signaling Technology. The antibodies for GST (MA4-004) and PAQR3 (PA5-24654, for human cells) were purchased from Thermo Scientific Pierce. The antibodies for Myc (9E10), GAPDH (sc-365062), His tag (sc-8036), β-actin (sc-47778), and PAQR3 (sc-161992, for mouse samples) were from Santa Cruz Biotechnology. The antibody for Beclin1 (Bethyl A302-567A) was used in immunoprecipitation. The antibodies for ATG5 (10181-2-AP) and VPS15 (17894-1-AP) were from Proteintech. Compound C, rapamycin, chloroquine (CQ), and antibodies for Flag (F3165), ATG7 (A2856) and ATG14L (A6358 for immunoblotting) were from Sigma-Aldrich. Antibodies for ATG14L (PD026 for immunoprecipitation), LC3 (PM036 for immunostaining), UVRAG (M160-3 for immunoblotting), and ATG7 (PM039 for immunoblotting) were from MBL International Corporation. The antibodies for GM130 (ab52649) was from Abcam. PAQR3 T32 phospho-specific antibody was produced by Signalway Antibody LLC (SAB, Shanghai, China). The peptides were synthesized by GL Biochem Ltd. (Shanghai, China) with the following sequences: control peptide, RKKRRQRRR; P21~40, RKKRRQRRRPVLVPRGIRLYTYEQIPGSL; P41~60, RKKRRQRRRKDNPYITDGYRAYLPSRLCI.

Co-immunoprecipitation and two-step co-immunoprecipitation

For co-immunoprecipitation (Co-IP) assays, cells were washed three times and then lysed with a mild lysis buffer [10 mM Tris, pH7.5, 2 mM EDTA, 100 mM NaCl, 1% NP-40, 50 mM NaF, 1 mM Na_3VO_4, and protease inhibitor cocktail (Roche)] for 30 min at 4℃. The homogenates were centrifuged for 30 min at 12,000 rpm at 4℃. 10% of the supernatant was harvested for Western blotting analysis as inputs, while the remaining cell lysate was incubated with primary antibodies overnight at 4℃. Protein A/G plus agarose (Genescript) was added at 4℃ for 2 h. The resulting beads were washed with IP buffer

for 5 times, followed by Western blotting analysis. For IP of skeletal muscles and liver, tissues was dissected and homogenized in lysis buffer containing 50 mM Tris (pH 7.9), 150 mM NaCl, 1 mM EDTA, 1% Triton X-100, proteinase inhibitor cocktail (Roche Applied Sciences) and halt phosphatase inhibitor cocktail (Thermo Scientific). The two-step co-IP assays were performed as previously reported (Harada et al, 2003; Rui et al, 2004).

Immunofluorescence staining, protein co-localization quantitation and fractionation of Golgi membranes

Confocal microscopy analysis was performed as previously reported (Feng et al, 2007). The Golgi and autophagosome marker were determined by immunostaining with antibodies against GM130 (Abcam) and LC3 (MBL) respectively. Nuclei were stained with Hoechst 33342 (Molecular Probes). The fluorescent secondary antibody for MEFs was Alexa Fluor 488 donkey anti-rabbit IgG, the fluorescent secondary antibodies for HeLa cells were Alexa Fluor 546 donkey anti-rabbit IgG. To examine autophagy under different conditions precisely, pictures in the same panel were taken under the same excitation conditions. The merged pictures were generated by LSM 5 IMAGE Browser (Zeiss, Germany) automatically. Co-localization was quantified by calculating Pearson's correlation coefficient value using the Coloc 2 plugin of ImageJ. Golgi membranes were isolated from the mouse liver as reported previously (Bartz et al, 2008; Wang et al, 2013; Wei & Seemann, 2009).

Gel filtration analysis

Gel filtration analysis was performed as described previously (Ma et al, 2014). In short, liver tissues were extracted and homogenized in ice-cold homogenization buffer (50 mM Tris-HCl, pH 7.5, 150 mM NaCl, 0.1% Triton X-100, 1 mM PMSF, complete protease inhibitor cocktail (Roche) and phosphatase inhibitors), and then followed by sonication for 2 min on ice. The homogenate was subjected to low-speed centrifugation at 17,000g for 5 min and then ultracentrifuged at 100,000g for 60 min. After pro-filtration with a 0.22 μm pore size hydrophilic polyethersulfone (PES) membrane, the resulting

supernatants were applied to a Superose 6 10/300 GL column using fast protein liquid chromatography (GE Healthcare) and eluted at a flow rate of 0.5 ml/min. The fractions were finally precipitated with trichloroacetic acid (TCA) and examined by immunoblotting.

LC−MS/MS analysis

For analysis of PAQR3 phosphorylation sites, bacterial purified His-tagged NH_2-terminal 71aa of PAQR3 was subjected to AMPK kinase assay *in vitro*. Then the protein sample was purified, and precipitated by trichloric acid followed by acetone washing. The pellets were solubilized and reduced in a buffer containing 7 M urea, 2 M thiourea, 10 mM HEPES, 1 mM sodium orthoranadate, 5 mM sodium fluoride, 5 mM β-glycerophosphate, and 10 mM DTT, pH 8.0, then alkylated with 50 mM iodoacetamide. After reducing urea concentration to 2 M, the samples were digested with trypsin (Promega, USA) at 37℃ (1:100 w/w) overnight. The digested peptide mixtures were acidified with trifluoroacetic acid (TFA) at 1% final concentration and desalted by reversed-phase C18 Sep-Pak cartridge (Millipore, USA). Phosphopeptides were enriched using TiO_2 beads (Titansphere, GL Sciences, Japan) in 80% acetonitrile (ACN) and 0.5% acetic acid in 3,4-dihydroxybenzoic acid solution. After a serial wash with buffer 1 (5 mM KH_2PO_4, 30% ACN, 350 mM KCl), buffer 2 (40% ACN, 0.5% acetic acid, 0.05% TFA) and buffer 3 (80% ACN, 0.5% acetic acid), the phosphorylated peptides were eluted first with 5% NH_4OH followed by 10% NH_4OH in 25% ACN. Eluted peptides were concentrated in a speedVac and desalted using C18 STAGE-tip. The samples were analyzed on an EASY-nLC1000 LC system (Thermo Scientific) coupled to the Q-Exactive mass spectrometer (Thermo Scientific). Peptides were loaded on an in-house packed C18-column (15 cm, 75 μm I.D., 2 μm particle size) with a gradient of 12%-32% buffer B (98% acetonitrile, 0.1% acetic acid) in 30 min followed by a 5 min wash with 95% buffer B. Full scan MS spectra were acquired at a resolution of 70,000 with an AGC target value of 3×10^6 and a maximum injection time of 100 ms. MS/MS spectra were acquired at a resolution of 17,500 with a target value of 1×10^5 and a maximum injection time of 50 ms. The raw files were processed by the MaxQuant software (version 1.5.3.8) searching against the Uniprot

database, with a variable modification of serine, threonine and tyrosine phosphorylation. For analyzing the stoichiometric binding partners of PAQR3, Myc-tagged PAQR3 immunoprecipitated from the PAQR3-reconstituted HeLa cells were eluted by Myc peptide and subjected to silver staining. Specific bands were exercised and digested in the gel with trypsin, and the resulting peptide mixtures were analyzed by LC-MS/MS. The MS/MS spectra were searched against the non-redundant human protein sequence database at the National Center for Biotechnology Information (NCBI).

Mouse behavioral studies

All mice used in behavioral testing experiment were housed in the same situation to avoid environmental biasing. The following tests were carried out on 11-month-old male PAQR3 knockout mice. The limb clasping phenotype was measured by suspending each mouse by its tail for 30 s and a clasping score of 0–3 was given as described previously (Cyr et al, 2003): 0, no clasping; 1, paw clenching and abnormal extension of the hindlimbs were noticed; 2, mild clasping (only fore or hind limbs press into the stomach); 3, severe clasping (both fore and hind limbs touch and press into the stomach). The accelerating rotarod test was performed on a standard accelerating rotarod device (Panlab, Harvard Apparatus) as previously described (Dang et al, 2006). Briefly, mice were trained to use the rotarod apparatus during a habituation trial at 4 rpm before testing. On the testing day, after mice were placed onto a horizontal rotating rod, the rotarod was accelerated from 4 to 40 rpm at a rate of 0.2 rpm/s. Mice were tested for two consecutive days, receiving three trials per day with 1 h intertribal interval. The time of mouse spent on the rotating rod until it fell off was recorded. Gait analysis was detected as previously described (Cyr et al, 2003). Briefly, the fore and hind paws of mice were painted with nontoxic red and blue paint respectively, and then the mice were allowed to walk across an uncovered corridor lined with paper. Paw prints were scanned using scanner and analyzed by measuring the stride length and gait width. Grip strength analysis was performed as previously described (Mandillo et al, 2008). Briefly, mice were handled by their tails and placed over the grid until all 4 paws grasped the grid of the grip strength test meter (BIOSEB; EB Instruments). The tail was then pulled in parallel with the mouse

body until the mouse released hold entirely. The maximum force was digitally displayed in grams. Five separate readings of each mouse were recorded and averaged.

References

Bartz R, Sun LP, Bisel B, Wei JH, Seemann J (2008) Spatial separation of Golgi and ER during mitosis protects SREBP from unregulated activation. *EMBO J* 27: 948-955

Cong L, Ran FA, Cox D, Lin S, Barretto R, Habib N, Hsu PD, Wu X, Jiang W, Marraffini LA, Zhang F (2013) Multiplex genome engineering using CRISPR/Cas systems. *Science* 339: 819-823

Cyr M, Beaulieu JM, Laakso A, Sotnikova TD, Yao WD, Bohn LM, Gainetdinov RR, Caron MG (2003) Sustained elevation of extracellular dopamine causes motor dysfunction and selective degeneration of striatal GABAergic neurons. *Proc Natl Acad Sci U S A* 100: 11035-11040

Dang MT, Yokoi F, Yin HH, Lovinger DM, Wang Y, Li Y (2006) Disrupted motor learning and long-term synaptic plasticity in mice lacking NMDAR1 in the striatum. *Proc Natl Acad Sci U S A* 103: 15254-15259

Feng L, Xie X, Ding Q, Luo X, He J, Fan F, Liu W, Wang Z, Chen Y (2007) Spatial regulation of Raf kinase signaling by RKTG. *Proc Natl Acad Sci U S A* 104: 14348-14353

Harada J, Kokura K, Kanei-Ishii C, Nomura T, Khan MM, Kim Y, Ishii S (2003) Requirement of the co-repressor homeodomain-interacting protein kinase 2 for ski-mediated inhibition of bone morphogenetic protein-induced transcriptional activation. *J Biol Chem* 278: 38998-39005

Jiang Y, Xie X, Zhang Y, Luo X, Wang X, Fan F, Zheng D, Wang Z, Chen Y (2010)

Regulation of G-protein signaling by RKTG via sequestration of the G betagamma subunit to the Golgi apparatus. *Mol Cell Biol* 30: 78-90

Ma B, Cao W, Li W, Gao C, Qi Z, Zhao Y, Du J, Xue H, Peng J, Wen J, Chen H, Ning Y, Huang L, Zhang H, Gao X, Yu L, Chen YG (2014) Dapper1 promotes autophagy by enhancing the Beclin1-Vps34-Atg14L complex formation. *Cell Res* 24: 912-924

Mali P, Yang L, Esvelt KM, Aach J, Guell M, DiCarlo JE, Norville JE, Church GM (2013) RNA-guided human genome engineering via Cas9. *Science* 339: 823-826

Mandillo S, Tucci V, Holter SM, Meziane H, Banchaabouchi MA, Kallnik M, Lad HV, Nolan PM, Ouagazzal AM, Coghill EL, Gale K, Golini E, Jacquot S, Krezel W, Parker A, Riet F, Schneider I, Marazziti D, Auwerx J, Brown SD, *et al* (2008) Reliability, robustness, and reproducibility in mouse behavioral phenotyping: a cross-laboratory study. *Physiol Genomics* 34: 243-255

Qin XF, An DS, Chen IS, Baltimore D (2003) Inhibiting HIV-1 infection in human T cells by lentiviral-mediated delivery of small interfering RNA against CCR5. *Proc Natl Acad Sci U S A* 100: 183-188

Rui Y, Xu Z, Lin S, Li Q, Rui H, Luo W, Zhou HM, Cheung PY, Wu Z, Ye Z, Li P, Han J, Lin SC (2004) Axin stimulates p53 functions by activation of HIPK2 kinase through multimeric complex formation. *EMBO J* 23: 4583-4594

Wang X, Wang L, Zhu L, Pan Y, Xiao F, Liu W, Wang Z, Guo F, Liu Y, Thomas WG, Chen Y (2013) PAQR3 modulates insulin signaling by shunting phosphoinositide 3-kinase p110alpha to the Golgi apparatus. *Diabetes* 62: 444-456

Wei JH, Seemann J (2009) The mitotic spindle mediates inheritance of the Golgi ribbon structure. *J Cell Biol* 184: 391-397

Zhang Y, Jiang X, Qin X, Ye D, Yi Z, Liu M, Bai O, Liu W, Xie X, Wang Z, Fang J, Chen Y (2010) RKTG inhibits angiogenesis by suppressing MAPK-mediated autocrine VEGF signaling and is downregulated in clear-cell renal cell carcinoma. *Oncogene* 29: 5404-5415

Zhong Y, Morris DH, Jin L, Patel MS, Karunakaran SK, Fu YJ, Matuszak EA, Weiss HL, Chait BT, Wang QJ (2014) Nrbf2 protein suppresses autophagy by modulating Atg14L protein-containing Beclin 1-Vps34 complex architecture and reducing intracellular phosphatidylinositol-3 phosphate levels. *J Biol Chem* 289: 26021-26037

Appendix Fig S1

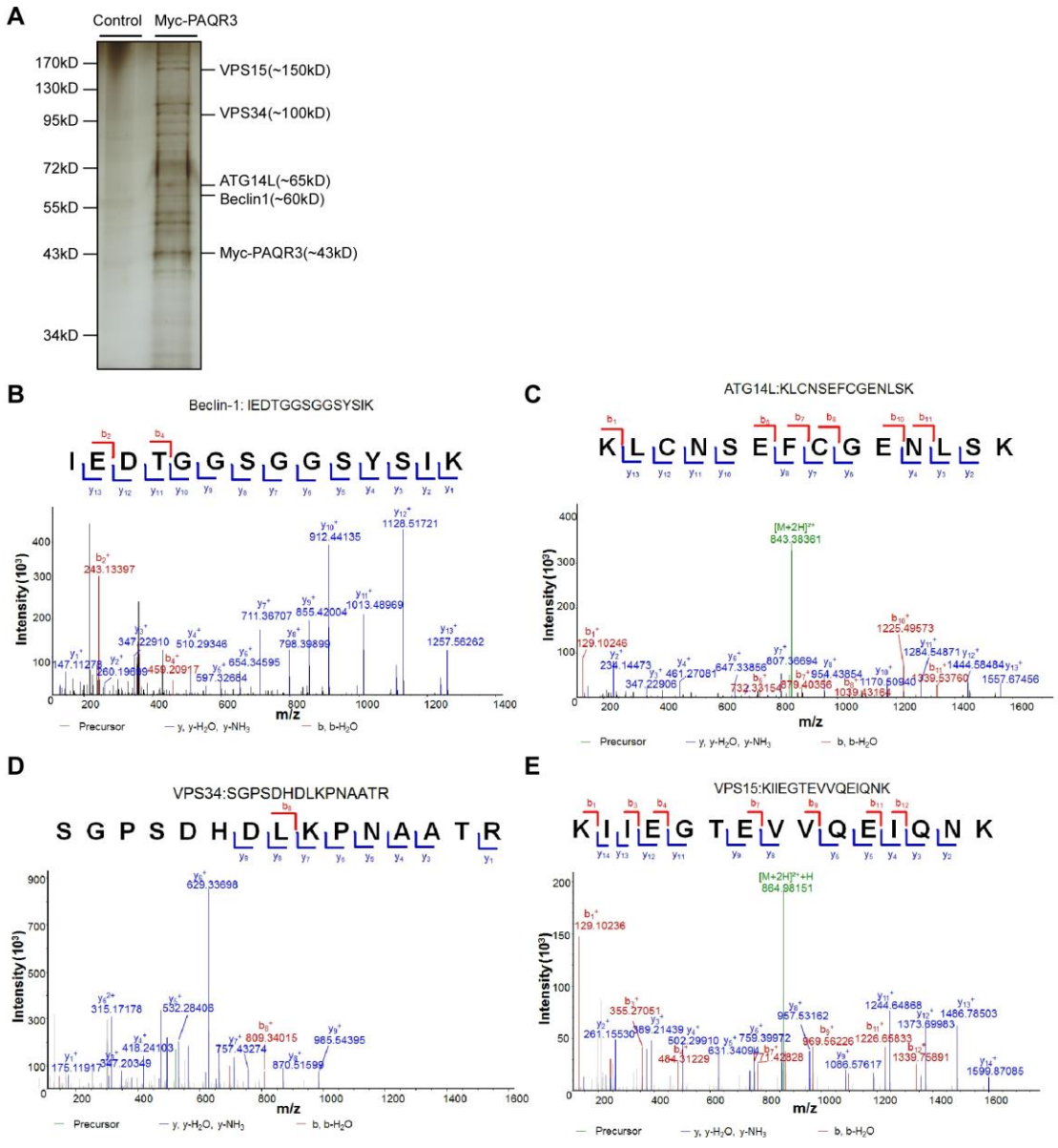

Appendix Fig S1. ATG14L-linked VPS34 complex is the binding partner of PAQR3.

(A) PAQR3-deficient HeLa cells were infected with lentivirus expressing Myc-tagged PAQR3, which was immunoprecipitated by an anti-Myc antibody. The associated proteins were eluted by a Myc peptide, and subjected to silver staining.

(B~E) Proteins in the gel bands were extracted and identified by mass spectrometry as indicated.

Appendix Fig S2

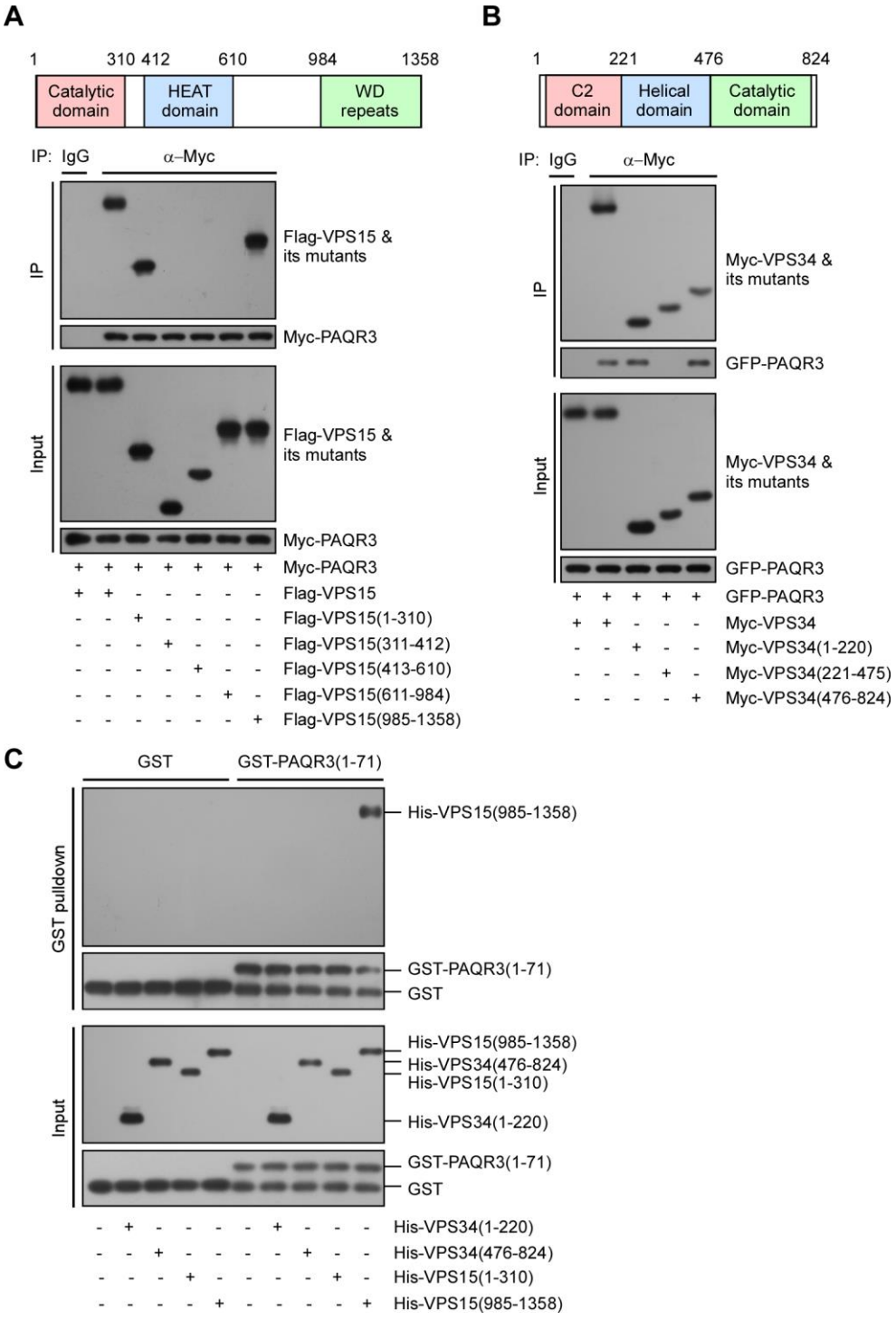

Appendix Fig S2. PAQR3 directly interacts with VPS15, but not VPS34.

(A) Different truncations of VPS15 were co-transfected with Myc-tagged PAQR3 into HEK239T cells as indicated, followed by immunoblotting (IB) and immunoprecipitation

(IP) analysis.

(B) GFP-tagged PAQR3 were co-transfected with different truncations of VPS34 into HEK239T cells as indicated, followed by IB and IP analysis.

(C) GST and GST-PAQR3 N71 (GST fused NH_2-terminal 71 aa of PAQR3) on glutathione agarose beads was mixed with purified His-tagged proteins as indicated. After incubation at 4 °C for 3 h, the samples were washed extensively and subjected to IB analysis.

Appendix Fig S3

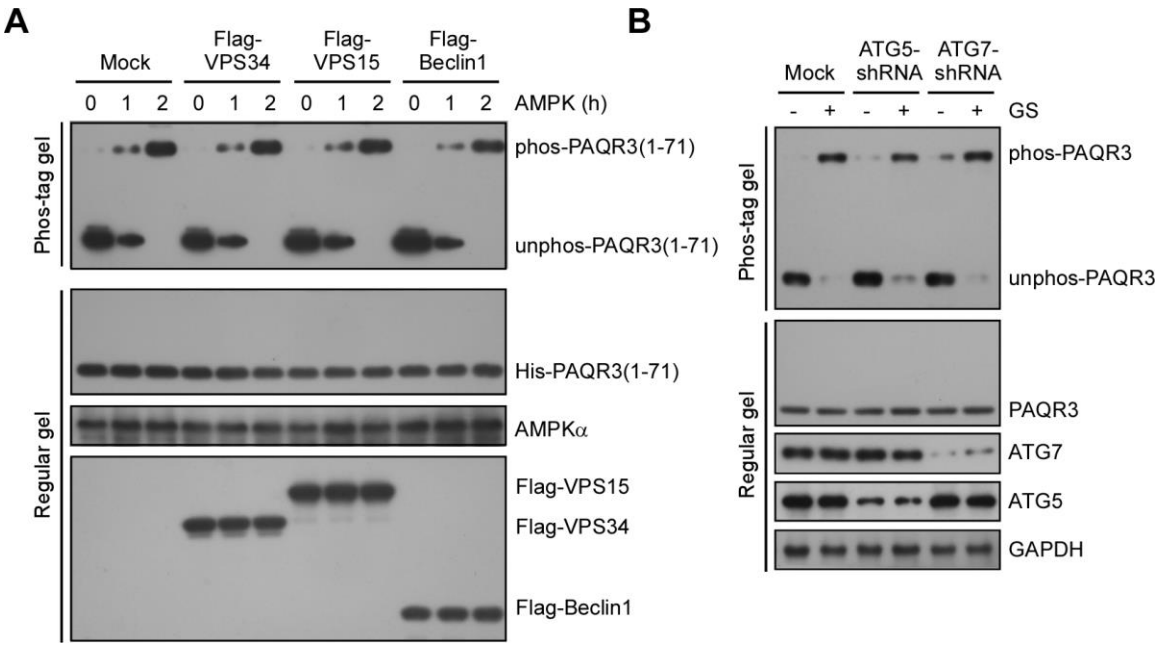

Appendix Fig S3. PAQR3 phosphorylation cannot be regulated by Beclin1, VPS15, VPS34 or autophagy *per se*.

(A) Bacterial purified His-tagged N-terminal 71 amino acid of PAQR3 was incubated with Flag-tagged VPS34, Flag-tagged VPS15 and Flag-tagged Beclin1 purified from HEK293T respectively. Then the complexes were incubated with AMPK for the indicated time *in vitro*. PAQR3 phosphorylation was examined by Phos-tag gel analysis.

(B) HeLa cells were transfected with ATG5 or ATG7 shRNA respectively. 48 h later, the cells were incubated under normal medium (NM) or glucose starvation (GS) for another 4 h. Whole cell lysates were analyzed by both Phos-tag gel and regular SDS-PAGE.

Appendix Fig S4

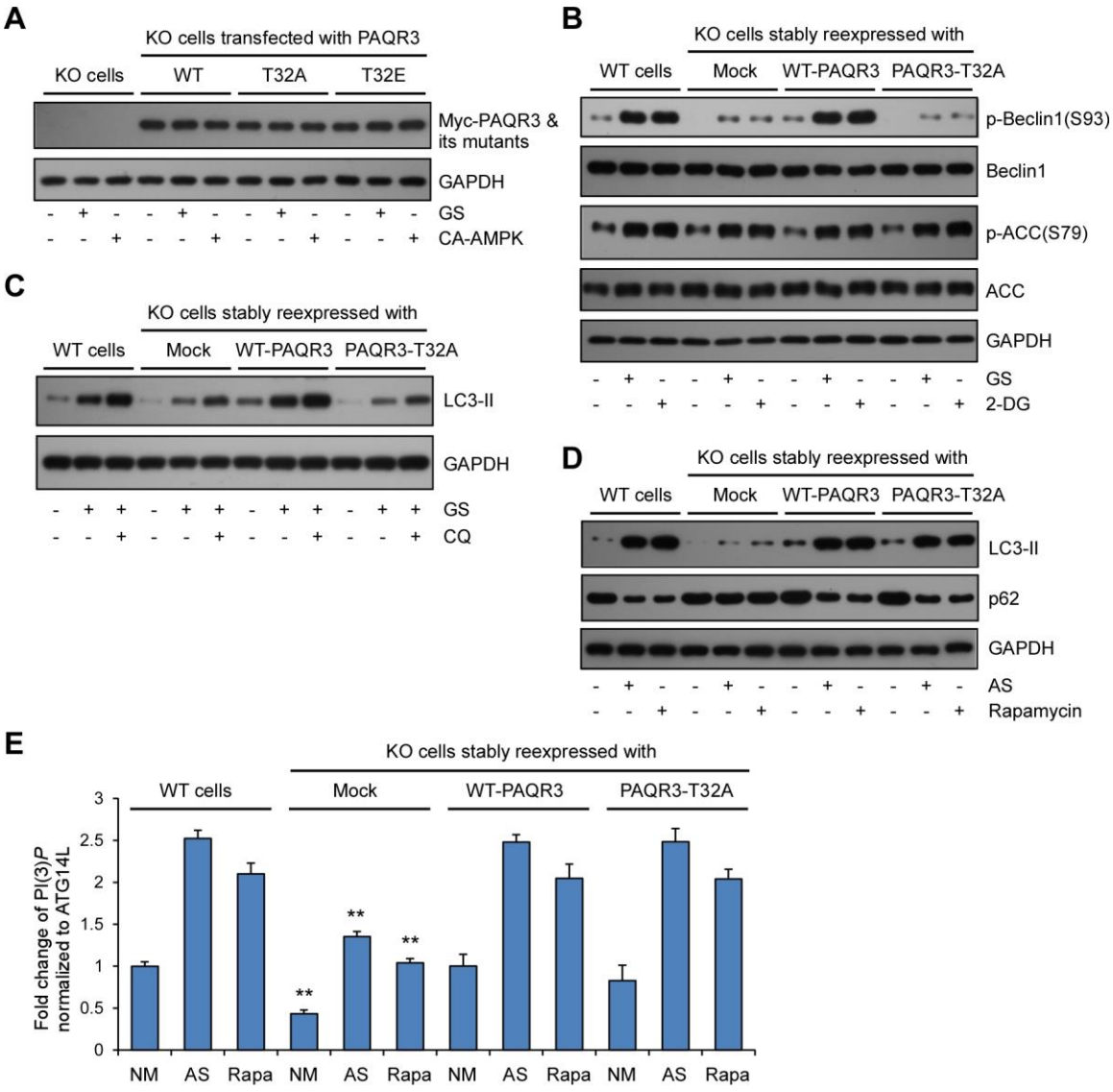

Appendix Fig S4. PAQR3 is not involved in amino acid depletion or rapamycin-induced autophagy.

(A) WT, T32A or T32E mutant PAQR3 were transfected into PAQR3 deficient HeLa cells. 10% of the cell lysates were subjected to immunoblotting (IB) analysis of PAQR3 expression.

(B) PAQR3-deficient HeLa cells were infected with lentivirus expressing WT or T32A PAQR3 respectively. After glucose starvation (GS) or 2-DG (25 mM) treatment for 1 h, the cell lysates were analyzed by IB with the indicated antibodies.

(C) PAQR3 deficient HeLa cells were infected with lentivirus expressing WT or T32A PAQR3. After GS in the absence or presence of 80 mM chloroquine (CQ) for 4 h, the cell lysates were harvested for IB analysis with indicated antibodies.

(D) PAQR3 knockout HeLa cells were infected with lentivirus expressing WT or T32A PAQR3. After amino acid starvation (AS) or rapamycin (50 nM) treatment for 4 h, the whole cell lysates were harvested for IB with indicated antibodies.

(E) PAQR3 deficient HeLa cells were infected with lentivirus expressing WT or T32A mutant PAQR3 respectively. After amino acid starvation (AS) or rapamycin (50 nM) treatment for 4 h, VPS34 complexes were immunopurified by ATG14L antibody, followed by VPS34 activity detection by a quantitative PI(3)*P* ELISA assay. The PI(3)*P* level was normalized to the amount of ATG14L ($n = 5$; $^{**}p < 0.01$ as compared to the first group with the same treatment).

Appendix Fig S5

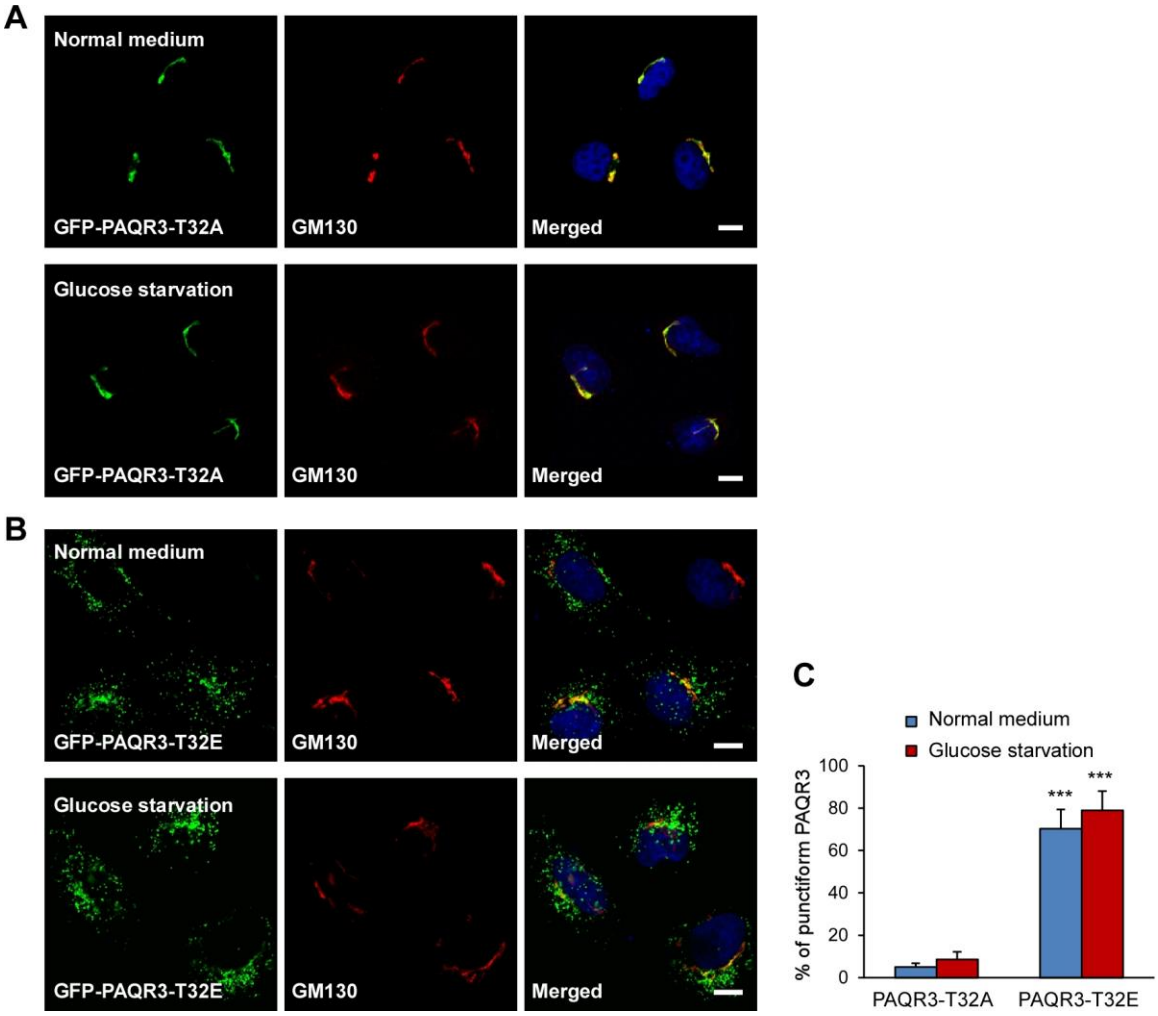

Appendix Fig S5. PAQR3 T32 phosphorylation is required for its punctiform distribution upon glucose starvation.

(A, B) PAQR3 T32A or T32E transfected HeLa cells were treated with or without glucose starvation (GS) for 4 h, the cells were then fixed for immunofluorescence staining with GM130 antibody. Scale bar: 10 μm.

(C) At least 100 cells were counted per experiment and the data represented the percentage of punctiform PAQR3 with or without glucose starvation from three independent experiments (*** for $p < 0.001$).

Appendix Fig S6

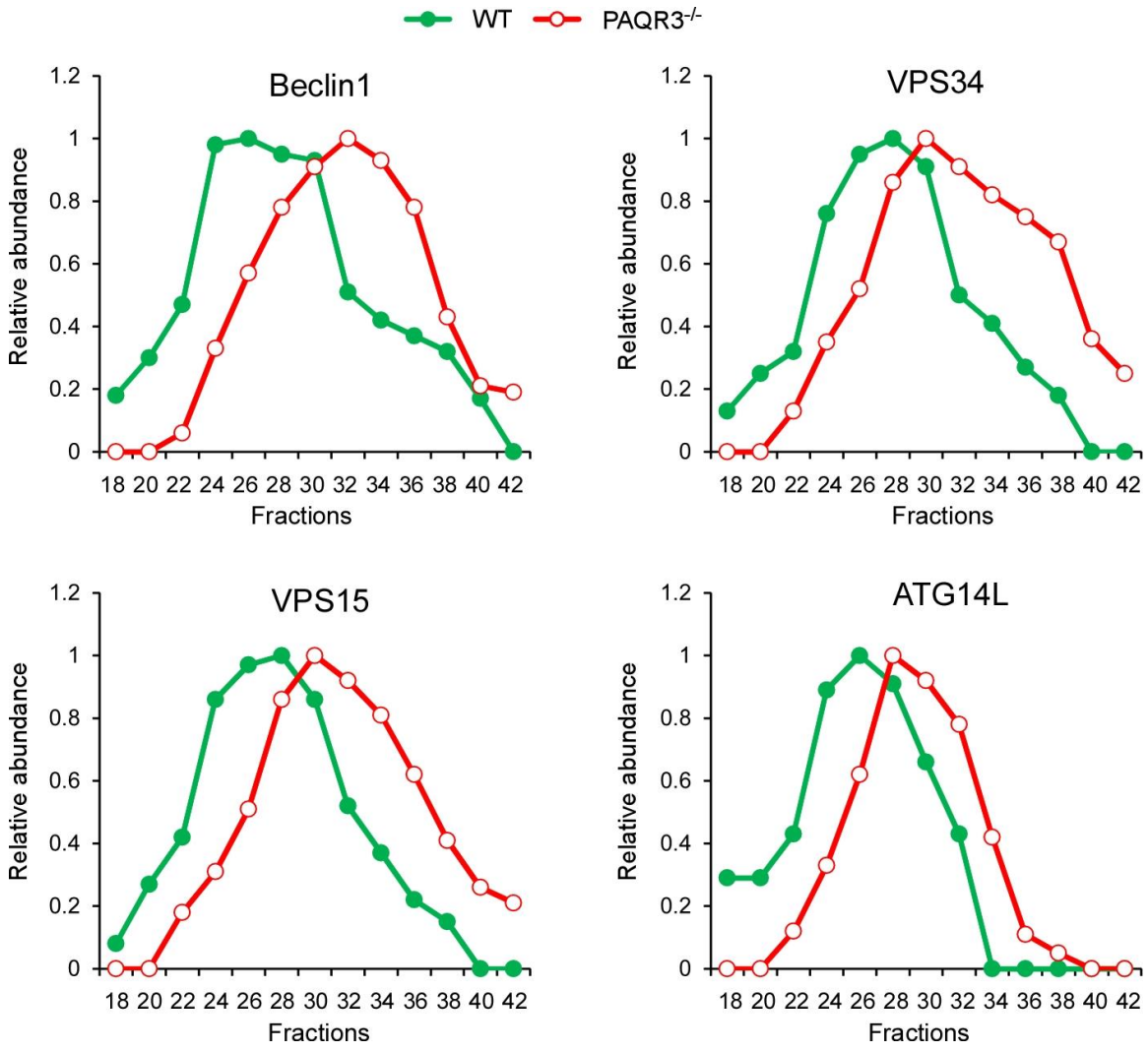

Appendix Fig S6. The components of ATG14L-linked VPS34 complex are shifted to lower molecular weight in PAQR3-deficient mice.

The relative distribution of each protein in different fractions after densitometry analysis of the blots in Figure 7H.

Appendix Fig S7

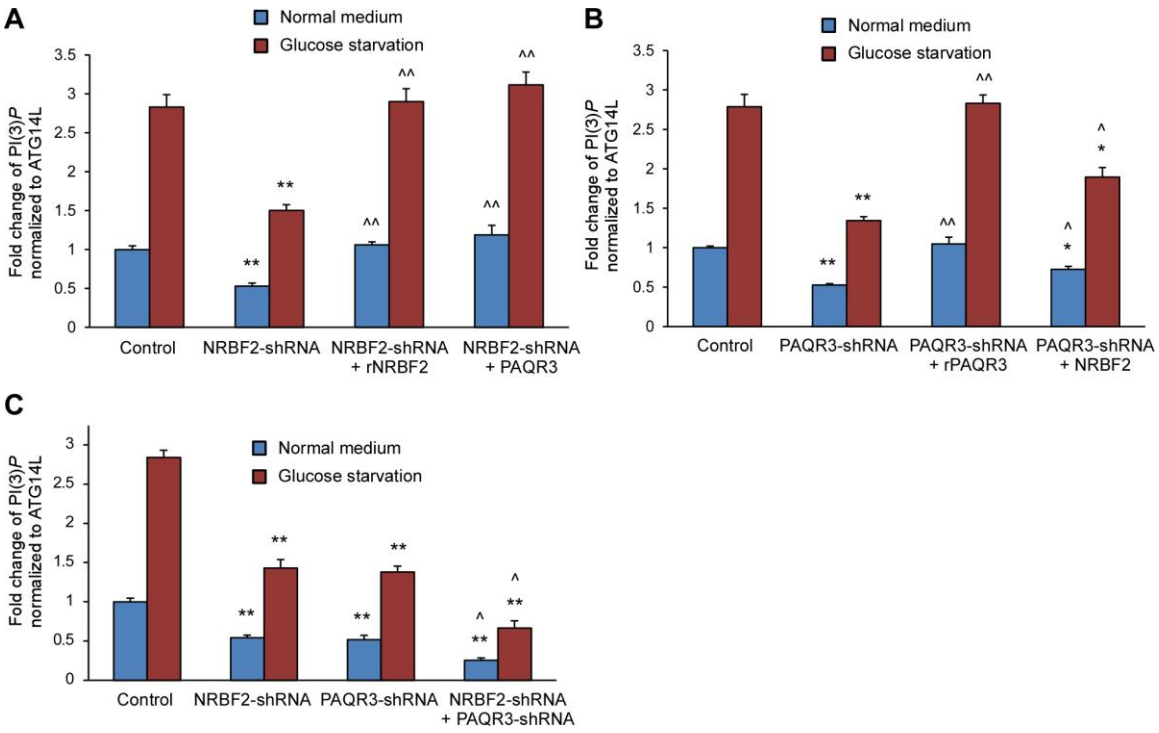

Appendix Fig S7. PAQR3 and NRBF2 are both required for modulating ATG14L-linked class III PI3K activity.

(A~C) (A) NRBF2-knockdown HeLa cells were infected with lentivirus expressing PAQR3 and shRNA-resistant NRBF2 respectively as indicated. (B) PAQR3-knockdown HeLa cells were infected with lentivirus expressing NRBF2 and shRNA-resistant PAQR3 respectively as indicated. (C) HeLa cells were infected with NRBF2- or PAQR3-knockdown lentivirus as indicated. After glucose starvation (GS) for 4 h, ATG14L-linked VPS34 complexes were immunoprecipitated from the cell lysates by ATG14L antibody. The PI(3)P level was determined by a quantitative ELISA assay. The PI(3)P level was normalized to the amount of ATG14L in this assay (n = 5; * for $p < 0.05$ and ** for $p < 0.01$ as compared with the first group with the same treatment; ^ for $p < 0.05$ and ^^ for $p < 0.01$ as compared with the second group with the same treatment).

Appendix Fig S8

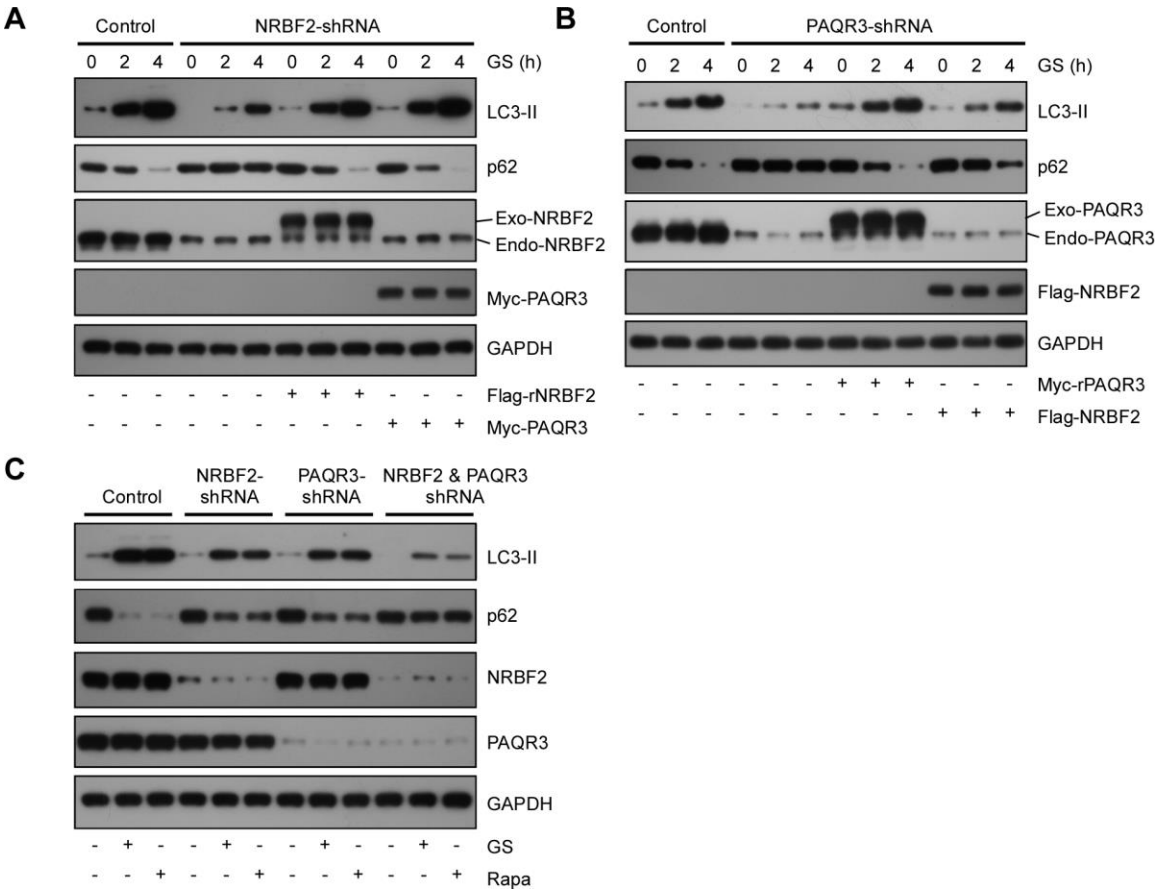

Appendix Fig S8. PAQR3 and NRBF2 are both necessary to coordinately regulate autophagic activity.

(A) NRBF2-knockdown HeLa cells were infected with lentivirus expressing PAQR3 and shRNA-resistant NRBF2 respectively. After glucose starvation (GS) for 2 h or 4 h, cell lysates were subjected to immunoblotting (IB) analysis with the indicated antibodies.

(B) PAQR3-knockdown HeLa cells were infected with lentivirus expressing NRBF2 and shRNA-resistant PAQR3 respectively. After glucose starvation (GS) for 2 h or 4 h, cell lysates were subjected to IB analysis with the indicated antibodies.

(C) HeLa cells were infected with NRBF2- or PAQR3-knockdown lentivirus as indicated. After glucose starvation or rapamycin (50 nM) treatment for 4 h, whole-cell lysates were harvested for IB analysis with indicated antibodies.

Appendix Fig S9

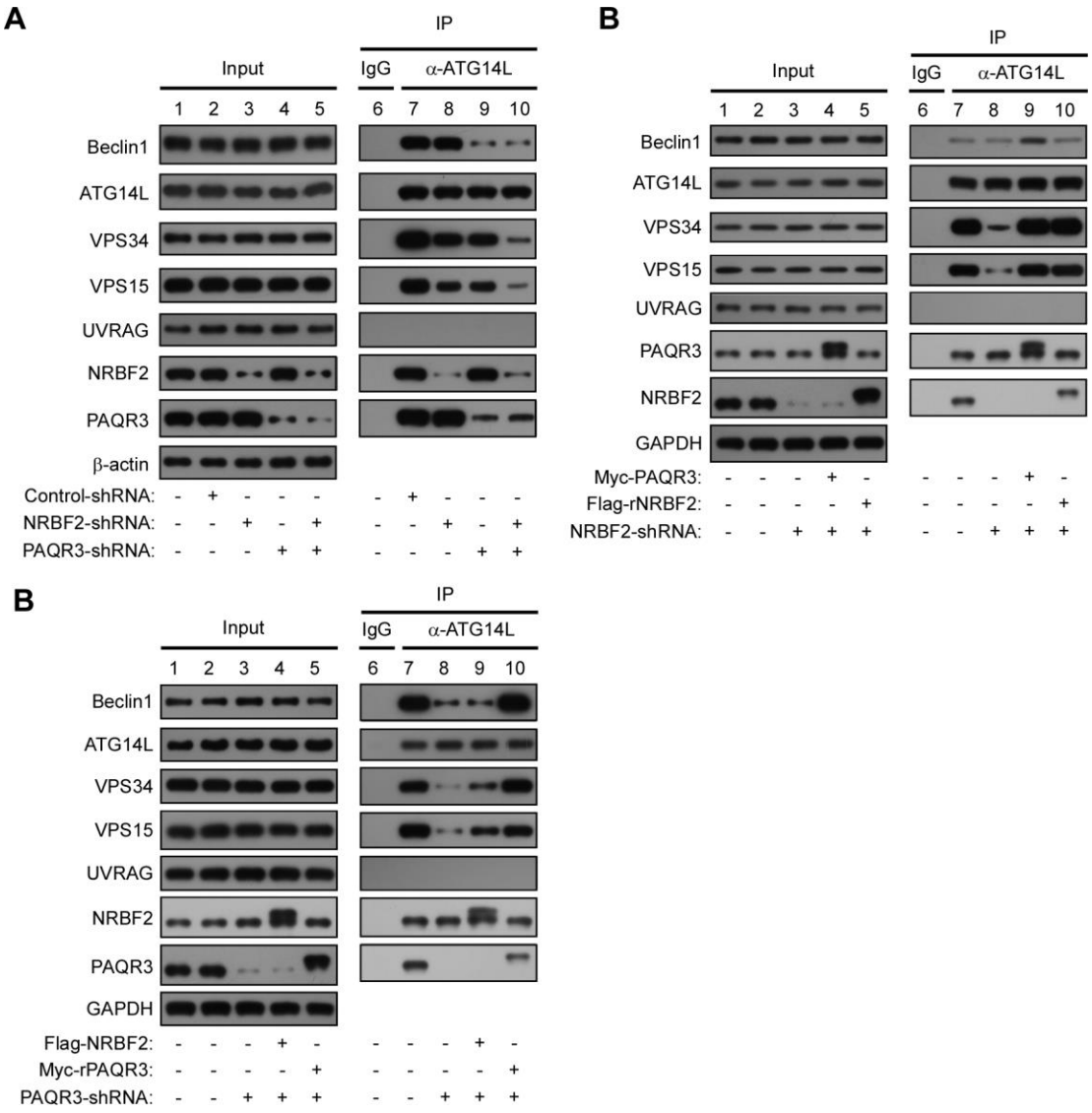

Appendix Fig S9. PAQR3 and NRBF2 are both required for ATG14L-linked VPS34 complex assembly.

(A) HeLa cells were infected with PAQR3- and NRBF2-knockdown lentivirus as indicated. The cell lysates were used for immunoblotting (IB) and immunoprecipitation (IP) analysis with the indicated antibodies.

(B) NRBF2-knockdown HeLa cells were infected with lentivirus expressing PAQR3 and shRNA-resistant NRBF2 respectively.

(C) PAQR3-knockdown HeLa cells were infected with lentivirus expressing NRBF2 and shRNA-resistant PAQR3 respectively. The cell lysates were used immunoblotting (IB) and immunoprecipitation (IP) with the indicated antibodies.